



ELSEVIER

Available online at [www.sciencedirect.com](http://www.sciencedirect.com)

SCIENCE @ DIRECT®

Composites: Part A 34 (2003) 1125–1131

**composites**

Part A: applied science  
and manufacturing

[www.elsevier.com/locate/compositesa](http://www.elsevier.com/locate/compositesa)

## A new mixed mode test for carbon/epoxy composite systems

Gregory D. Tracy<sup>a</sup>, Paolo Feraboli<sup>b,\*</sup>, Keith T. Kedward<sup>b</sup>

<sup>a</sup>Raytheon Infrared Operations, Goleta, CA 93107, USA

<sup>b</sup>Department of Mechanical Engineering, University of California, Santa Barbara, CA 93106, USA

Accepted 26 April 2003

### Abstract

The present research examines analytically and experimentally the mixed mode interlaminar fracture toughness of a resin film infused (RFI) carbon fiber/epoxy laminate, namely a IM7-AS4/3501-6 hybrid composite system. The inability to develop representative interlaminar failure in composites with current mixed mode test configurations motivated this particular investigation. The paper is part of a more extensive research effort concerned with the effects of stitching upon the mixed mode fracture toughness of a RFI composite.

A new mixed mode test configuration is suggested, the Single Leg Four Point Bend (SLFPB), which provides a robust method with small specimens and a simple apparatus. Closed form fracture mechanics-based strain energy release (SERR) calculations have been established for this configuration. Finite element analysis was conducted to validate the closed form solution. Results show a very good agreement between analytical solutions, numerical simulation and the newly designed SLFPB experimental test.

© 2003 Elsevier Ltd. All rights reserved.

*Keywords:* Mixed mode delamination; B. Fracture toughness

### 1. Introduction

The primary concern with polymer composites is delamination failure, which is debonding of adjacent plies, since the through-thickness properties of composite laminates are typically matrix dominated and therefore, much weaker than the fiber dominated in-plane properties. Inter-ply delaminations are usually initiated in one of three ways; (i) by process related defects, (ii) damage due to impact (handling or service related), (iii) direct or induced out-of-plane loads. Interlaminar shear or normal stresses are of particular importance in laminated composite structures, due to their highly anisotropic nature. Interlaminar stresses originate because of a mismatch in the mechanical properties between individual laminae within the laminate and develop at the free edge and at local discontinuities such as notches, ply-drops, bonded and bolted joints, or when the laminate is subject to hygro-thermal variations. These stresses need to be evaluated for structural applications and many

authors feel that delamination growth is the fundamental issue in the evaluation of laminated composite systems for durability and damage tolerance. In-service delaminations often occur under complex load conditions and mixed mode failure phenomena are not yet well understood.

The laminate of interest in this paper is a hybrid composite comprised of IM7 and AS4 fibers in a relatively brittle 3501-6 epoxy matrix. The lay-up considered is  $[\pm 45/0_2/90/0_2/\pm 45]_{ns}$  with  $n = 4, 6$ , which yields a [44/44/11] ply percentage in the  $0/\pm 45/90^\circ$  orientation, respectively. The hybrid laminate calls for IM7 fibers in the  $0^\circ$  plies, and AS4 in the  $45$  and  $90^\circ$  plies.

While Mode I testing is usually performed with the aid of the Double Cantilever Beam fixture (DCB), and Mode II testing with the End Notch Flexure setup, a review of existing mixed mode test methods was undertaken to identify the most suitable for this particular composite system [1]. Popular mixed mode tests are Crack Lap Shear [2,3], Unsymmetric Double Cantilever Beam [2,4], Single Leg Bend (SLB) [7–9], and Four Point Bend (FPB) [10–13], but the most universally accepted is the Mixed Mode Bend [2,5,6].

Each test has advantages and drawbacks. Table 1 lists the relative merits and disadvantages of each test while Fig. 1

\* Corresponding author. Tel.: +1-805-893-3381; fax: +1-805-407-1123.

E-mail addresses: [pmc@engineering.ucsb.edu](mailto:pmc@engineering.ucsb.edu) (P. Feraboli); [gregory\\_d\\_tracy@raytheon.com](mailto:gregory_d_tracy@raytheon.com) (G.D. Tracy); [kedward@engineering.ucsb.edu](mailto:kedward@engineering.ucsb.edu) (K.T. Kedward).

Table 1  
Mixed mode test method comparison

Test method	Advantages	Disadvantages
Crack lap shear	Simple fixture and coupon geometry; small crack opening displacement; constant mode ratio	Requires non-linear numerical analysis; due to large rotations at crack tip; different ply lay-ups needed for different mode ratios
Unsymmetric DCB	Simple coupon geometry; closed-form solution exists	Requires complex fixture; requires bonded hinged tabs
Mixed mode bend	Simple coupon geometry; variable mode mix ratio	Requires complex fixture; requires bonded hinged tabs; complex data reduction techniques
Single leg bend	Simple fixture and coupon geometry; simple closed-form solution	Mode ratio changes with crack length; different coupon geometry needed for different mode ratios
Four point bend	Simple fixture and coupon geometry; simple closed-form solution; constant mode ratio	Two cracks growing simultaneously at different rates; different coupon geometry needed for different mode ratios

shows a side-to-side comparison of specimen geometry and loading configurations. Other less used test methods include Edge Delamination Tension, Fixed Ratio Mixed Mode, Arcan and Variable Mixed Mode [2].

Due to disadvantages associated with the existing tests, none of them was considered to be an optimal mixed mode test solution for the evaluation of this material. As a result, a new test fixture was developed to incorporate features from both the SLB and FPB tests. The new Single Leg Four Point Bend (SLFPB) (Fig. 2) test eliminates both the double crack growth problem inherent to the FPB and the change in mode ratio as a function of crack length typical of the SLB. It does not require a complex test apparatus, nor does it need a non-linear numerical analysis. The SLFPB test utilizes a small test coupon and a simple test fixture while providing a relatively simple method of obtaining controlled, mixed mode crack propagation.

This paper will evaluate the SLFPB test as an alternative to current mixed mode testing methods. A fracture mechanics-based analytic strain energy release rate (SERR) solution that accounts for material anisotropy has been previously established for the SLFPB configuration.

The analytical model will be first verified using a highly meshed finite element model (FEM), then compared to experimentally obtained data.

2. Analytical investigation

The fracture mechanics equations for  $G_I$  and  $G_{II}$  SERR expressions [14] for an isotropic material subjected to FPB loading are

$$G_I = \frac{3M^2}{Eh^3}, \quad G_{II} = \frac{9M^2}{4Eh^3} \tag{1}$$

where  $h$  is the single leg thickness,  $M$  is the resulting moment per unit width, and  $E$  is Young's modulus. A rescaling technique has been used to determine the SERR for orthotropic laminates [14,15]. For the particular case where the leg thickness is half the total thickness,  $h = H/2$ , the Mode I and Mode II SERR can be expressed as

$$G_I = b_{11}n\lambda^{-3/4}\phi^2, \quad G_{II} = b_{11}n\lambda^{-1/4}\theta^2 \tag{2}$$

where  $\phi$  and  $\theta$  take the form

$$\phi = \lambda^{3/8}M\sqrt{\frac{3}{nh^3}}, \quad \theta = \lambda^{1/8}M\sqrt{\frac{9}{4nh^3}} \tag{3}$$

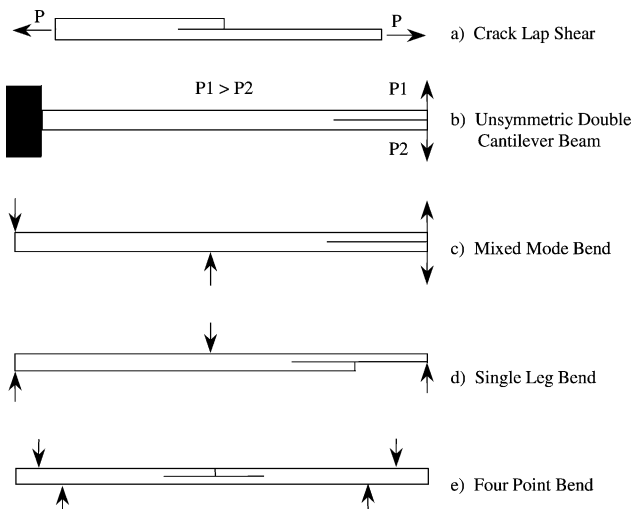


Fig. 1. Common Mixed Mode test configurations.

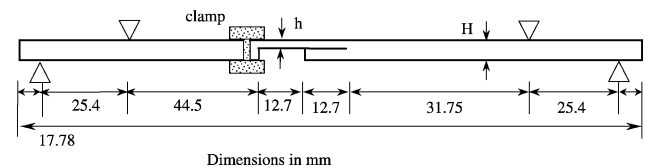


Fig. 2. Single Leg Four Point Bend coupon configuration.

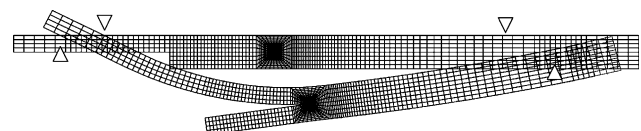


Fig. 3. ABAQUS Single Leg Four Point Bend finite element model.

Table 2  
Material properties as measured and calculated

$E_1 = 69.7$ GPa (10.11 Msi)	$E_2 = 36.5$ GPa (5.3 Msi)	$E_{flex} = 66.2$ GPa (9.60 Msi)
$G_{12} = 19.8$ GPa (2.867 Msi),	$G_{13} = 5.86$ GPa (0.85 Msi),	$G_{23} = 4.482$ GPa (0.65 Msi)
$\nu_{12} = 0.388$	$\nu_{13} = 0.3$	$\nu_{23} = 0.3$

and the non-dimensional parameters  $n$ ,  $\rho$  and  $\lambda$  are measures of the material anisotropy

$$n = \sqrt{\frac{\rho + 1}{2}}, \quad \rho = \frac{2b_{12} + b_{66}}{2\sqrt{b_{11}b_{22}}}, \quad \lambda = \frac{b_{11}}{b_{22}} \quad (4)$$

and can be evaluated for plane strain conditions using Hooke’s law

$$\epsilon_{ij} = \sum_{j=1,2,6} b_{ij}\sigma_{ij}, \quad \text{where } b_{ij} = s_{ij} - \frac{s_{i3}s_{j3}}{s_{33}}, \quad (5)$$

$i, j = 1, 2, 6$

The mode mix ratio can be determined using the following equation [14]:

$$\frac{\theta}{\phi} = \frac{\sqrt{3}}{2} \lambda^{-1/4} \quad (6)$$

For the material in question, the mode mixity has been calculated as 1.03, approximately 50% Mode I and 50% Mode II.

An ABAQUS FEM of the SLFPB test configuration has been generated to confirm the analytical solution. Two

different thicknesses were evaluated; 54-ply ( $H = 8.64$  mm (0.34 in.)) and 36-ply ( $H = 5.59$  mm (0.22 in.)). A total of 28,231 nodes and 26,229 eight-node plane strain elements were used. The FEM incorporates a focused mesh crack tip that allows the determination of the total SERR using the  $J$ -integral calculated over 10 contours around the crack tip. SERR values were calculated for the SLFPB configuration over a range of 0–11.12 kN (0–2500 lb) applied load, which was the load range used in the experimental investigation.

The model is depicted in Fig. 3, where the mesh is shown in the undeformed and deformed states (exaggerated for clarity). The geometry of the model is slightly different from the test specimen, the difference being the overhang of material under one of the supporting rollers. The notch was machined in the test coupon for sake of simplicity, avoiding the burden of machining the remaining dead material before the crack tip. It can be seen that such an assumption has no effect on the resulting moment at the crack tip. The remaining dimensions used in the FEA are the same as the test coupon.

The flexural modulus of the laminate was previously determined through a series of experiments [16], while the remaining material properties were calculated by means of lamination theory ( $E_1, E_2, G_{12}, G_{13}, G_{23}, \nu_{12}, \nu_{13}, \nu_{23}$ , see Table 2) and were then incorporated into the ABAQUS FEM input data.

The analytic and FEM were evaluated in plane strain conditions for two different specimen thicknesses: 36-ply ( $H = 5.59$  mm (0.22 in.)) and 54-ply ( $H = 8.64$  mm

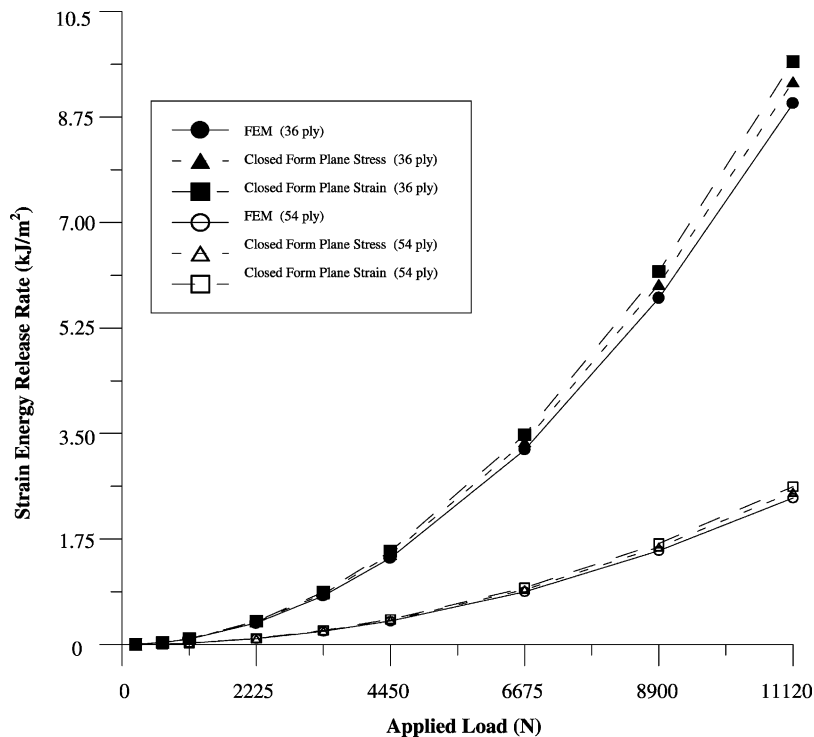


Fig. 4. Closed Form (CF) SERR vs. FEM SERR comparison.

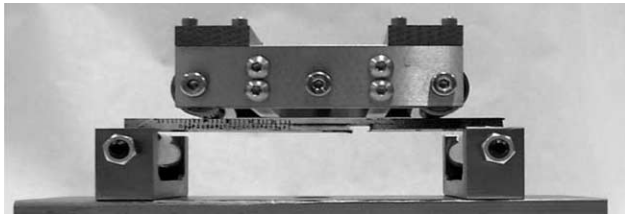


Fig. 5. Picture of SLFPB test fixture.

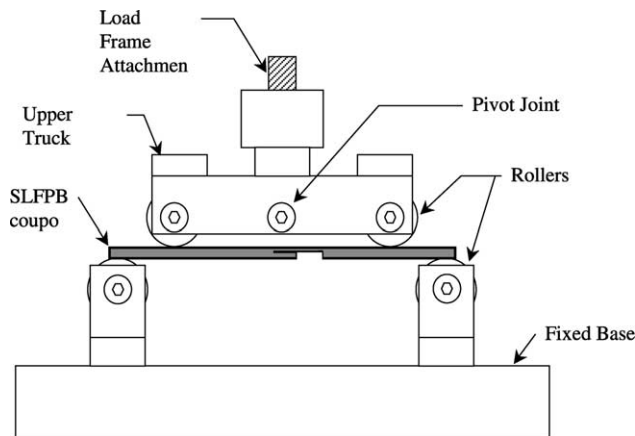


Fig. 6. Diagram of SLFPB test fixture.

(0.34 in.)). The FEM SERR values were compared to analytic solutions and are graphically depicted in Fig. 4.

The comparison of the closed form solution and FEM data yields that the analytic plane stress results are uniformly 4% higher than FEM while the analytic plane strain results are consistently 7% higher than FEM.

Given the consistency and the relative accuracy of the analytic results compared to the FEM, it can be concluded that both the plane stress and plane strain analytic solutions give a reasonably accurate description of the mixed mode SERR for both the 54-ply and 36-ply laminates studied.

### 3. Experimental investigation

Proof-of-concept testing of SLFPB mixed mode fracture test has been completed. As mentioned previously, the laminate tested has a  $(\pm 45/0_2/90/0_2/\pm 45)_{ns}$  stacking sequence, with  $n = 4, 6$  for a total thickness of 5.59 mm (0.22 in.) and 8.64 mm (0.34 in.). The two thicknesses were tested to determine if there was any dependence in SERR on specimen thickness. The specimen geometry and loading configuration are shown in Fig. 2.

The 54-ply coupons were cut from a  $305 \times 305 \text{ mm}^2$  ( $12 \times 12 \text{ in.}^2$ ) plate; while the 36-ply coupons came from a separate  $711 \times 711 \text{ mm}^2$  ( $28 \times 28 \text{ in.}^2$ ) panel.

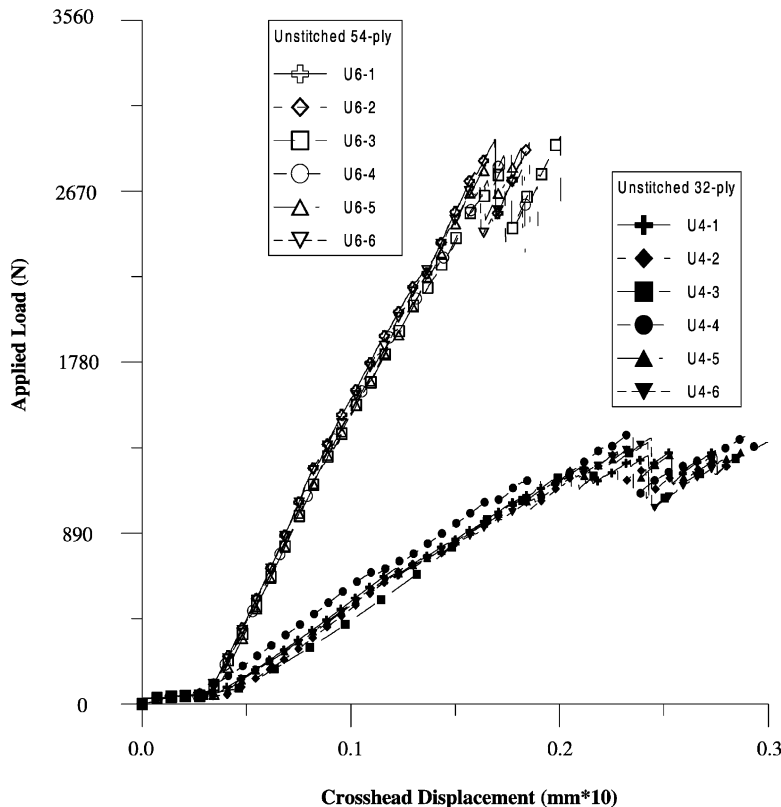


Fig. 7. Applied load vs. crosshead displacement for 36-ply and 54-ply specimens.

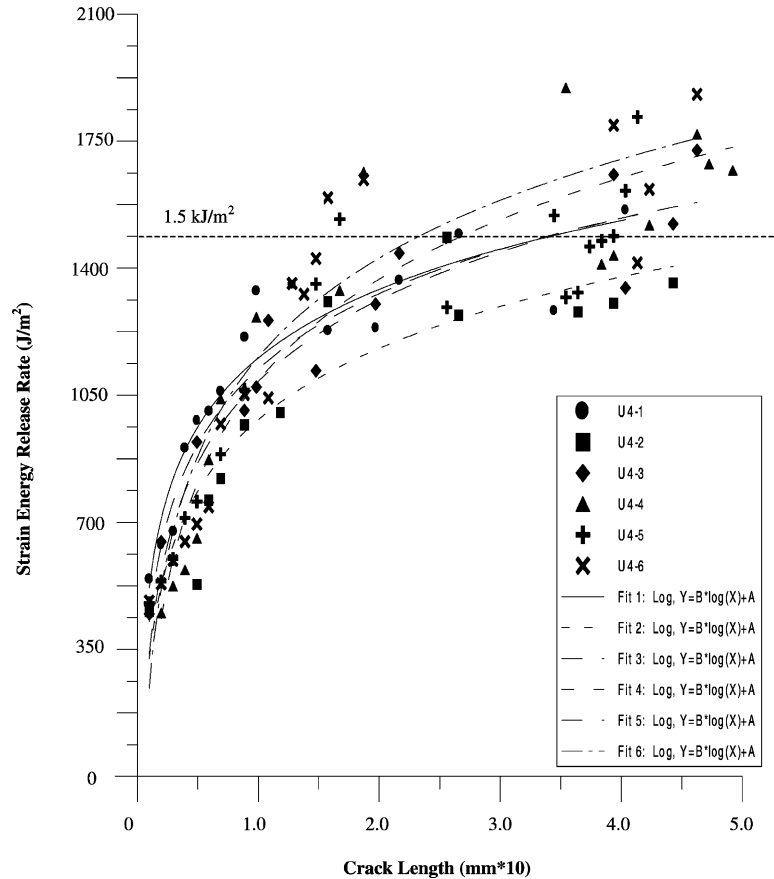


Fig. 8. 36-Ply strain energy release rate vs. crack length.

The delamination initiation region was obtained by embedding a strip of 25.4 mm (1 in.) wide and 5  $\mu\text{m}$  thick of Teflon at the mid-plane.

A total of six specimens per thickness were cut to a nominal 25.4 mm (1 in.) width and 177.8 mm (7 in.) length using a water-cooled circular saw with a diamond-coated tip. A 12.7 mm (0.5 in.) notch was machined into the surface to create the single leg.

Due to the asymmetric configuration of the SLFPB specimen, a test fixture was developed to ensure that equal force was applied to the two contact points on the upper surface. The upper loading truck is allowed to pivot about the centerline, as shown in Figs. 5 and 6, and compensates the loading asymmetry that appears as the crack advances, thus allowing to maintain a region of constant moment between the inner rollers.

In order to prevent the crack from propagating on the other side of the notch, a crack suppressing operation was performed by means of a simple clamp.

The tests were run on an Instron 1123 test machine under displacement control at a crosshead feed rate of 0.508 mm/min (0.02 in./min). Each coupon was painted white on the side and then scribed so that a monoscope could be used to visually observe crack growth.

The experimental test results for the 54-ply and 36-ply specimens were consistent, and crack growth was controllable in both cases. Crack growth occurred in a ‘stick slip’ manner, the crack advancing at finite increments, which is the reason for the single, finite data points that characterize the SERR vs. crack length plot. The load–displacement curves (Fig. 7) show that the maximum applied load for the 54-ply coupons averaged 2.67 kN (600 lb ft), while for the 36-ply coupons was consistently in the 1.34 kN (300 lb ft) range. Maximum load for the 54-ply specimens was thus approximately double that of the 36-ply, but the crack length at maximum displacement was significantly less. The reason for this is due to the greater cross-sectional moment of inertia, hence increased bending resistance of the thicker specimens.

The SERRs were calculated from the load data using the previously described analytic method. The SERR vs. crack length curves (Figs. 8 and 9) show that the SERR at which steady state crack propagation occurred for the 54-ply material ( $\sim 1.7 \text{ kJ/m}^2$  [10 in. lb ft/in.<sup>2</sup>]) was slightly higher than for the 36-ply material ( $\sim 1.5 \text{ kJ/m}^2$  [9 in. lb ft/in.<sup>2</sup>]). Previous single mode fracture toughness testing of similar (AS4/3501 and IM7/3501) material has produced Mode I SERR values between 0.1 and 0.3  $\text{kJ/m}^2$  and Mode II SERR values between 0.6 and 1.5  $\text{kJ/m}^2$  [17,18].

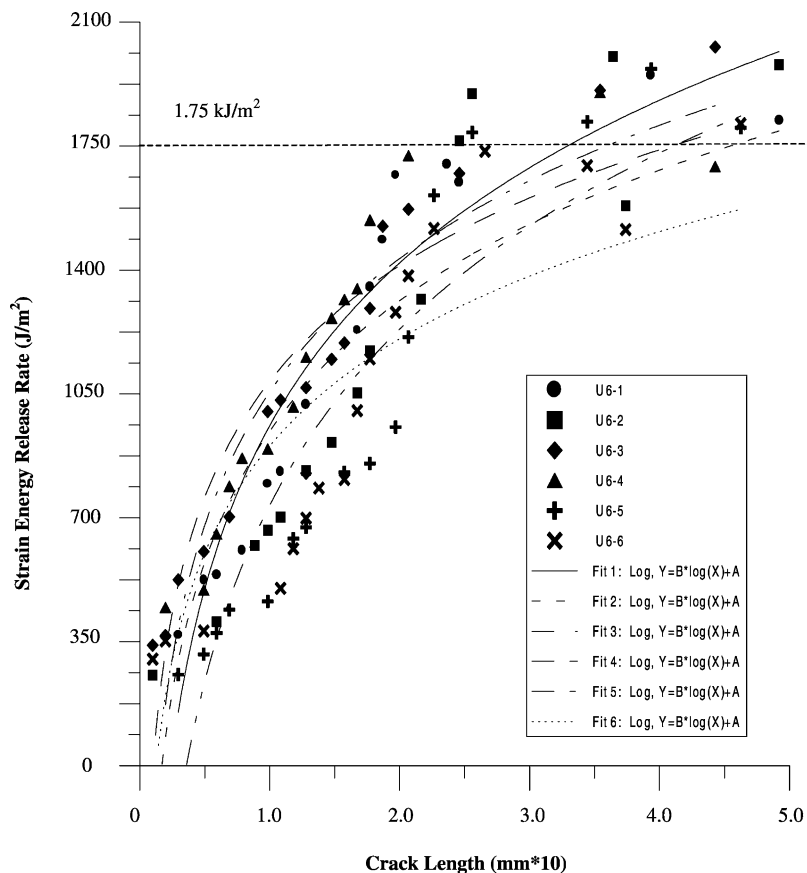


Fig. 9. 54-Ply strain energy release rate vs. crack length.

#### 4. Conclusions

A new Mixed Mode Test has been developed, the SLFPB, which has been shown to be a simple yet effective method. Previously determined closed form fracture mechanics-based SERR solutions for this configuration have been verified through finite element modeling. A prototype SLFPB mixed mode test fixture was manufactured for the testing of a hybrid IM7-AS4/3501-6 composite system. Very good agreement was obtained for all three approaches. It was furthermore shown that the SERR at which steady state crack propagation occurred for the 54-ply specimens ( $1.750 \text{ kJ/m}^2$ ), was slightly higher than the 36-ply ( $1.576 \text{ kJ/m}^2$ ), therefore suggesting a slight influence of the specimen thickness on the SERR.

#### Acknowledgements

This research was funded in part by NASA through the Boeing Company in support of the Advanced Composite Technology program. The ACT program evaluated the use of advanced stitched/RFI composite laminates as

the primary structural material for the next generation of commercial transport aircraft.

#### References

- [1] O'Brien TK. Interlaminar fracture toughness: the long and winding road to standardization. *Composites, Part B (Engng)* 1998;29B(1): 57–62.
- [2] Reeder JR, Crews JH. Mixed mode bending method for delamination testing. *AIAA J* 1990;28(7):1270–6.
- [3] Russell AJ, Street KN. Moisture and temperature effect on the mixed mode fracture of unidirectional graphite/epoxy. *ASTM STP* 876; 1985. 349–70.
- [4] Sundararaman V, Davidson BD. Unsymmetric double cantilever beam test for interfacial fracture toughness determination. *Int J Solids Struct* 1997;34(7):799–817.
- [5] Reeder JR, Crews JH. Redesign of mixed mode bending delamination test to reduce nonlinear effects. *J Compos Tech Res* 1992;14(1): 12–19.
- [6] Kinloch AJ, Yayla P, Wang Y, Williams JG. Mixed mode delamination of fibre composite materials. *Compos Sci Tech* 1993; 47(3):225–37.
- [7] Yoon SH, Hong CS. Modified end notched flexure specimen for mixed mode interlaminar fracture in laminated composites. *Int J Fract* 1990;43:R3–R9.

- [8] Davidson BD, Sundararaman V. A single leg bending test for interfacial fracture toughness determination. *Int J Fract* 1996;78: 193–210.
- [9] Sundararaman V, Davidson BD. New test methods for determining fracture toughness as a function of mode mix for bimaterial interfaces. *ASME* 1995;EEP-11/MD-64:141–54.
- [10] Charalambides PG, Lund J, Evans AG, McMeeking RM. A test specimen for determining the fracture resistance of bimaterial interfaces. *J Appl Mech* 1989;56:77–82.
- [11] Charalambides PG, Cao H, Lund J, Evans AG. Development of a test method for measuring the mixed mode fracture resistance of bimaterial interfaces. *Mech Mater* 1990;8:269–83.
- [12] Charalambides PG. Steady state mechanics of delamination cracking in laminated ceramic–matrix composites. *J Am Ceram Soc* 1991; 74(12):3066–80.
- [13] Feraboli P, Kedward KT. Four-point bend interlaminar shear testing of uni- and multi-directional carbon/epoxy composite systems. *Composites, Part A* 2003; in press.
- [14] Suo Z, Bao G, Fan B, Wang TC. Orthotropy rescaling and implications for fracture in composites. *Int J Solids Struct* 1991; 28(2):235–48.
- [15] Bao G, Suo Z, Ho S, Fan B. The role of material orthotropy in fracture specimens for composites. *Int J Solids Struct* 1992;29(9): 1105–16.
- [16] Tracy GD. PhD Dissertation. University of California, Santa Barbara; 2001
- [17] O'Brien TK. Composite interlaminar shear fracture toughness, GIIC: shear measurement or sheer myth? *ASTM STP* 1330; 1998. p. 3–18.
- [18] Daniel IM, Ishai O. *Engineering mechanics of composite materials*. New York: Oxford University Press; 1993.